Appl Phys B (2010) 99: 579–584
DOI 10.1007/s00340-009-3864-6

Applied Physics B
Lasers and Optics

On the longitudinal polarization of non-paraxial electromagnetic fields

R. Martínez-Herrero · P.M. Mejías · A. Manjavacas

Received: 24 September 2009 / Revised version: 25 November 2009 / Published online: 14 January 2010

Abstract Within the framework of the angular plane-wave spectrum of the electromagnetic field, the general form is given for the freely-propagating beams, exact solution of the Maxwell equations, that closely approach (in an algebraic sense) to a purely-longitudinal vectorial distribution at some transverse plane. In the rotationally symmetric case, such a field is written as the combination of radial and longitudinal components, whose propagation can be analysed independently. Several illustrative examples are also considered.

1 Introduction

Although the polarization of an electromagnetic plane wave is purely transversal, any field with finite beam width exhibits a longitudinal component upon propagation [1]. In particular, the global description of non-uniformly polarized beams has been investigated in detail in the paraxial case (see, for example, [2, 3]). In the last years, however, longitudinal-polarization-dominant fields are attracting increasing attention, and a number of applications of the longitudinal polarization have been reported. They range from second-harmonic generation [4, 5] and fluorescent imaging [6] to Raman spectroscopy [7] and electron acceleration [8], to mention some of them. Furthermore, several procedures have been proposed to enhance such longitudinal component [9–12]: for instance, by focusing radially polarized radiation [10]. This is of special interest, for example, when radially polarized laser light is used for material processing [13].

In order to investigate the propagation of electromagnetic beams with significant longitudinal component, different approaches have been reported in the literature [14–19]. Among them, the complex-source-point model [17] and the vector diffraction theory using the Hertz vectors [15, 18, 19] are traditional methods to determine and propagate electric fields obeying the Maxwell equations.

In the present work we also consider longitudinal-polarization-enhanced fields, but they are studied from a different perspective, namely, on the basis of the angular plane-wave spectrum [20–23]. In this connection, it was introduced some years ago the concept of electromagnetic field "closest" (understood in an algebraic sense) to a given (realistic or hypothetical) transverse vectorial distribution [3, 24–26]. We refer to this class of beam as the closest field (CF) associated to a vector function at a transverse plane. Apart from their algebraic meaning, the CFs have been shown to represent exact solutions of the Maxwell equations, valid in the paraxial and non-paraxial regimes. The CF formalism is here applied to the analysis of certain electromagnetic fields whose amplitudes of the radial and longitudinal components are comparable (as takes place, for example, at sharp focusing).

More specifically, attention is focused on the CF associated to a pure longitudinal vectorial distribution at some plane. It should be noted that such kind of distribution does not satisfy the Maxwell equations, on the contrary to that fulfilled by its associated CF: It provides an exact solution and, in addition, represents the field algebraically closest to such ideal (but unrealistic) purely longitudinal distribution.

R. Martínez-Herrero · P.M. Mejías (✉)
Departamento de Óptica, Facultad de Ciencias Físicas,
Universidad Complutense de Madrid, 28040 Madrid, Spain
e-mail: pmmejias@fis.ucm.es
Fax: +34-91-3944673

A. Manjavacas
Instituto de Óptica, CSIC, Serrano 121, 28006 Madrid, Spain

The present paper is then arranged as follows. In the next section the formalism and several key definitions are introduced. In Sect. 3 the concept of CF and its algebraic meaning is recalled. Section 4 considers the CF associated to a purely longitudinal vectorial distribution at a transverse plane. The special but significant case of rotationally symmetric angular spectrum is analysed. To illustrate the above results, several examples are discussed in Sect. 5. Finally, the main conclusions are summarized in Sect. 6.

2 Formalism and key definitions

Let us consider a freely propagating monochromatic electromagnetic beam whose behavior is inferred from the Maxwell equations (in the Gauss system)

$$\nabla \times \boldsymbol{H} + ik\boldsymbol{E} = 0, \tag{1a}$$

$$\nabla \times \boldsymbol{E} - ik\boldsymbol{H} = 0, \tag{1b}$$

$$\nabla \cdot \boldsymbol{E} = 0, \tag{1c}$$

$$\nabla \cdot \boldsymbol{H} = 0, \tag{1d}$$

where vectors $\boldsymbol{E}$ and $\boldsymbol{H}$ involve the spatial structure of the electric and magnetic fields, respectively, and $k = 2\pi/\lambda$ denotes the wave number (λ being the wavelength). As is well known, the electric field can be expressed in terms of its angular plane-wave spectrum, namely,

$$\boldsymbol{E}(x, y, z) = \int \tilde{\boldsymbol{E}}(u, v, z) \exp\bigl[ik(xu + yv)\bigr]\, du\, dv, \tag{2}$$

and a similar expression for the magnetic part. In (2) $\tilde{\boldsymbol{E}}$ represents the spatial Fourier transform of the field $\boldsymbol{E}$, and we have chosen z as the direction of propagation of the beam. Neglecting the contribution of the evanescent waves, the general expression for $\tilde{\boldsymbol{E}}$, fulfilling the Maxwell equations, can formally be written in the form [3]

$$\tilde{\boldsymbol{E}}(\rho, \phi, z) = \tilde{\boldsymbol{E}}_0(\rho, \phi) \exp\bigl(ikz\sqrt{1-\rho^2}\bigr), \tag{3}$$

where ρ and ϕ denote polar coordinates related to the transverse Cartesian Fourier-transform variables (α, β) through the equations $\alpha = \rho\cos\phi$, $\beta = \rho\sin\phi$. To avoid any possible confusion, from now on, Greek-case letters refers to coordinates in the Fourier-transform space.

Let us now write the angular spectrum $\tilde{\boldsymbol{E}}_0$ [cf. (3)] in the form [3]

$$\tilde{\boldsymbol{E}}_0(\rho, \phi) = a(\rho, \phi)\boldsymbol{e}_1(\phi) + b(\rho, \phi)\boldsymbol{e}_2(\rho, \phi), \tag{4}$$

where $\boldsymbol{e}_1$ and $\boldsymbol{e}_2$ are the unitary vectors

$$\boldsymbol{e}_1 = (\sin\phi, -\cos\phi, 0), \tag{5a}$$

$$\boldsymbol{e}_2 = \bigl(\sqrt{1-\rho^2}\cos\phi, \sqrt{1-\rho^2}\sin\phi, -\rho\bigr), \tag{5b}$$

and

$$a(\rho, \phi) = \tilde{\boldsymbol{E}}_0 \cdot \boldsymbol{e}_1, \tag{6a}$$

$$b(\rho, \phi) = \tilde{\boldsymbol{E}}_0 \cdot \boldsymbol{e}_2. \tag{6b}$$

It is clear from these equations that functions $a(\rho, \phi)$ and $b(\rho, \phi)$ can be understood as the projection of $\tilde{\boldsymbol{E}}_0$ onto the vectors $\boldsymbol{e}_1$ and $\boldsymbol{e}_2$, respectively. The directions of vectors $\boldsymbol{e}_1$ and $\boldsymbol{e}_2$ should then be considered as reference axes (defining a plane) with respect to which the vector $\tilde{\boldsymbol{E}}_0$ is decomposed. In addition, (1c) gives

$$\tilde{\boldsymbol{E}}_0(\rho, \phi) \cdot \boldsymbol{s}(\rho, \phi) = 0, \tag{7}$$

where

$$\boldsymbol{s}(\rho, \phi) = \bigl(\rho\cos\phi, \rho\sin\phi, \sqrt{1-\rho^2}\bigr), \quad \rho \in [0, 1], \tag{8}$$

denotes a unitary vector indicating the propagation direction of each plane wave. It is important to note that $\boldsymbol{s}$, $\boldsymbol{e}_1$ and $\boldsymbol{e}_2$ form a triad of mutually orthogonal unit vectors.

3 Closest field and its algebraic meaning

We will now recall the concept of field *closest* (in an algebraic sense) to a vector function at a certain plane [3]. The starting point would be a certain vectorial distribution $\boldsymbol{f}(x, y)$ at some transverse plane, say, $z = 0$. Such function can be suggested, for instance, either from its easy-to-use analytical properties or from its potential applications. The problem arises if $\boldsymbol{f}(x, y)$ does not fulfill the Maxwell equations, and, consequently, it cannot represent a realistic light field. Instead of using $\boldsymbol{f}(x, y)$, we could then handle the so-called closest field associated of $\boldsymbol{f}$, defined as the electric-field solution of the Maxwell equations that is best fitted, in an algebraic sense, to the vector $\boldsymbol{f}$.

To clarify what this means let us write $\boldsymbol{f}$ in terms of its angular plane-wave spectrum $\tilde{\boldsymbol{f}}$, namely,

$$\boldsymbol{f}(x, y) = \int_0^1 \int_0^{2\pi} \tilde{\boldsymbol{f}}(\rho, \phi) \times \exp\bigl[ik\rho(x\cos\phi + y\sin\phi)\bigr]\rho\, d\rho\, d\phi, \tag{9}$$

where the evanescent waves have again been neglected. As follows from the previous section, function $\boldsymbol{f}$ would represent an electric-field solution at plane $z = 0$ provided its associated spectrum $\tilde{\boldsymbol{f}}$ belongs to the (two-dimensional) subspace S generated by $\boldsymbol{e}_1$ and $\boldsymbol{e}_2$. But, in general, an arbitrary function $\tilde{\boldsymbol{f}}$ does not fulfill this condition.

It can be shown, however, that the electric field $\boldsymbol{E}_f$ given by [3]

$$(\boldsymbol{E}_f)_{\text{closest}} = \int_0^1 \int_0^{2\pi} \bigl[(\tilde{\boldsymbol{f}} \cdot \boldsymbol{e}_1)\boldsymbol{e}_1 + (\tilde{\boldsymbol{f}} \cdot \boldsymbol{e}_2)\boldsymbol{e}_2\bigr] \times \exp(ik\boldsymbol{r} \cdot \boldsymbol{s})\rho\, d\rho\, d\phi, \tag{10}$$

is always a true solution of the Maxwell equations. But $(\tilde{\boldsymbol{f}} \cdot \boldsymbol{e}_1)\boldsymbol{e}_1 + (\tilde{\boldsymbol{f}} \cdot \boldsymbol{e}_2)\boldsymbol{e}_2$ just represents the projection of $\tilde{\boldsymbol{f}}$ onto the 2D subspace S. Accordingly, the projection of a vector $\boldsymbol{v}$ onto a plane provides the vector (contained in such plane) closest to $\boldsymbol{v}$ (in this algebraic sense). Accordingly, $\boldsymbol{E}_f$ [defined by (10)] constitutes the closest field (in the above sense) associated to $\tilde{\boldsymbol{f}}$.

Three further remarks should finally be noted:

1. Vector $\boldsymbol{v}(\rho,\phi) = (\tilde{\boldsymbol{f}} \cdot \boldsymbol{e}_1)\boldsymbol{e}_1 + (\tilde{\boldsymbol{f}} \cdot \boldsymbol{e}_2)\boldsymbol{e}_2$ is formally similar to $\tilde{\boldsymbol{E}}_0$, expressed by (4) and (6);
2. Equation (10) allows to determining the field $\boldsymbol{E}_f$ propagated into free space;
3. The concept of closest field applies for paraxial and non-paraxial cases.

4 Closest field associated to a purely longitudinal vectorial distribution

Attention will now be focused on the ideal case of a purely longitudinal vectorial distribution at a transverse plane, i.e. a vector $\boldsymbol{f}$ whose transverse components equal zero at some initial plane [3]. As we mentioned in the first section, this polarization structure is not realizable because it does not satisfy the Maxwell equations. Instead, we will consider the CF associated to such longitudinal distribution.

Note first that, in the present case, the angular plane-wave spectrum $\tilde{\boldsymbol{f}}$ takes the form

$$\tilde{\boldsymbol{f}}(\rho,\phi) = \big(0, 0, f_0(\rho,\phi)\big). \tag{11}$$

On this basis, the CF follows from direct application of (10): since $\tilde{\boldsymbol{f}} \cdot \boldsymbol{e}_1 = 0$, the field $\boldsymbol{E}_f$ propagates according with the law

$$\boldsymbol{E}_f = -\int_0^1\int_0^{2\pi} \rho f_0(\rho,\phi)\boldsymbol{e}_2 \exp(ik\boldsymbol{r}\cdot\boldsymbol{s})\rho\, d\rho\, d\phi, \tag{12}$$

which is valid for any function $f_0(\rho,\phi)$. It is clear from (12) that $\boldsymbol{E}_f$ does not preserve the pure longitudinal character of the generating vectorial distribution $\tilde{\boldsymbol{f}}$: In fact, $\boldsymbol{E}_f$ involves transverse and longitudinal components. However, it is not difficult to show that the magnetic-field counterpart is purely transverse to the z-axis, i.e. its longitudinal component equals zero.

In the particular but important case in which $f_0(\rho,\phi)$ exhibits rotational symmetry, i.e. $f_0(\rho,\phi) = f_0(\rho)$, the field $\boldsymbol{E}_f$ transforms into the expression

$$\boldsymbol{E}_f = iF_R(R,z)\boldsymbol{u}_R(\theta) + F_z(R,z)\boldsymbol{u}_z, \tag{13}$$

where, for the sake of convenience, we have used cylindrical coordinates, $\boldsymbol{u}_R$ and $\boldsymbol{u}_z$ denote the unit vectors in the radial and longitudinal directions, respectively, and

$$F_R(R,z) = -2\pi\int_0^1 \rho f_0(\rho)\sqrt{1-\rho^2}J_1(kR\rho) \times \exp\big(ikz\sqrt{1-\rho^2}\big)\rho\, d\rho, \tag{14a}$$

$$F_z(R,z) = 2\pi\int_0^1 \rho^2 f_0(\rho)J_0(kR\rho) \times \exp\big(ikz\sqrt{1-\rho^2}\big)\rho\, d\rho. \tag{14b}$$

The particularly simple form of the right-hand side of (13) allows to splitting out this kind of fields in terms of purely radial and longitudinal components, whose propagation can then be studied in a separate way. We can thus evaluate in an easy way the relative contribution of both components to the global field, as will be apparent in the example discussed in the following section. We also see at once from (13) and (14) that this CF, associated to a pure longitudinal-polarization distribution, exhibits rotational symmetry around the z-axis (as expected), and its transverse polarization is always radial at any beam cross section upon free propagation. Such a property can be thought as a supplementary analytical support to the well-known result of achieving a significant longitudinal component by focusing radially polarized light [10].

Furthermore, on the z-axis ($R = 0$), this CF reduces to

$$\boldsymbol{E}_f(R=0,z) = F_z(0,z)\boldsymbol{u}_z, \tag{15}$$

and the field only shows a longitudinal component.

5 Application to several examples

To illustrate the above analysis, let us first consider the Gaussian case, in which the angular spectrum obeys a Gaussian distribution, that is,

$$f_0(\rho) = \exp\left(-\frac{\rho^2}{D^2}\right), \tag{16}$$

where D is a constant (proportional to the divergence at the far field), closely connected with the beam width ω_0 through the relation $D = 1/k\omega_0$. It should be noted that this Gaussian function refers to the longitudinal component only [cf. (11)]. This represents an essential difference with regard to the conventional Gaussian case, in which the Gaussian distribution involves transverse components. Further details of the closest field associated to a transverse Gaussian function can be found, for instance, in Ref. [24].

The strength of the contributions of the radial and longitudinal components of the CF associated to the spectrum given by (16) is qualitatively described (pseudo-colored)

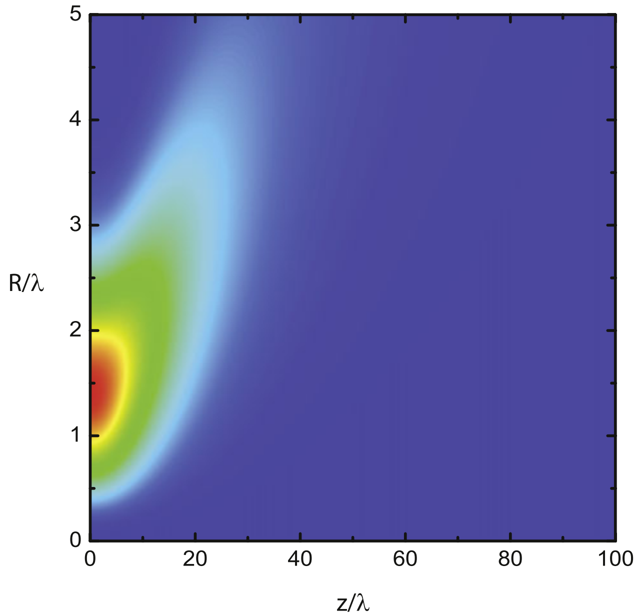

Fig. 1 Representation (in pseudo-color) of $|F_R|^2$ in a plane (R, z) for the example defined by (11) and (16). In the figure, $\omega_0 = \lambda$ and $D = \frac{\lambda}{2\pi\omega_0}$. The beam propagates from left to right and exhibits rotational symmetry around the z-axis. *Red colors* indicate higher values and *blue*—the lower ones

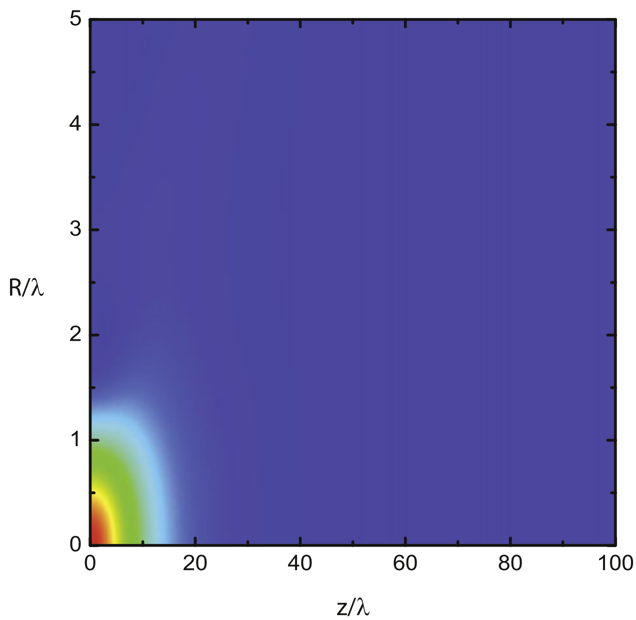

Fig. 2 The same as in Fig. 1 but now for $|F_z|^2$

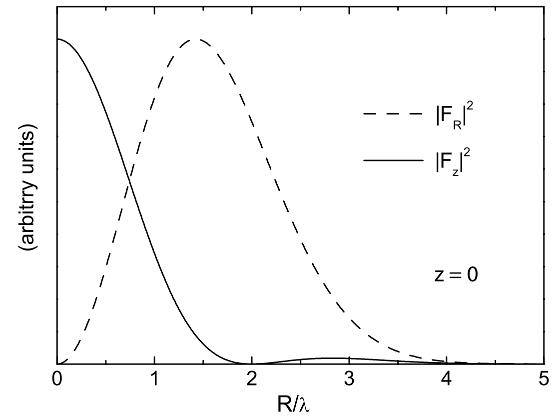

Fig. 3 Plot of $|F_z|^2$ (*continuous line*) and $|F_R|^2$ (*dashed line*) at the initial plane $z = 0$

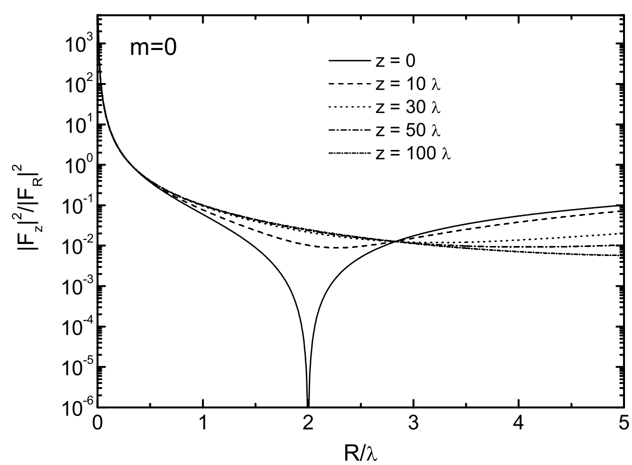

Fig. 4 Propagation of the ratio $\frac{|F_z|^2}{|F_R|^2}$ at several transverse planes. The value $z = 0$ corresponds to the initial plane. In abscissas, the radial distance to the z-axis is given in units of λ. In ordinates, the value 1 means that the two components (radial and longitudinal) have the same strength. Other characteristics observed in the figure are pointed out in the main text

in Figs. 1 and 2. In these figures (computed for the value $\omega_0 = \lambda$) the propagation distance $z = 100\lambda$ has been chosen because it corresponds to the so-called diffraction length $d = \omega_0^2/\lambda$. The red color indicates the regions where the respective field component is more significant. We thus see that the longitudinal component of the polarization predominates for points close enough to the z-axis.

The transverse behavior at the initial plane $z = 0$ is plotted in Fig. 3. Note that the longitudinal component vanishes at a ring (around the z-axis) whose radius equals 2λ.

For comparative purposes, Fig. 4 represents the ratio $\frac{|F_z|^2}{|F_R|^2}$ for several transverse planes at different propagation distances. Consequently, the curves show the relative weight of both components: Ordinate values higher than 1 means that the longitudinal polarization predominates. Otherwise, the radial component is more important.

From this figure, four main characteristics should be remarked:

1. In a small region around the z-axis (say, $R \leq 0.5\lambda$), all the curves nearly match. In other words, for this type of fields, propagation does not alter in a significant way the relative weight of the longitudinal component in the neighborhood of the z-axis.

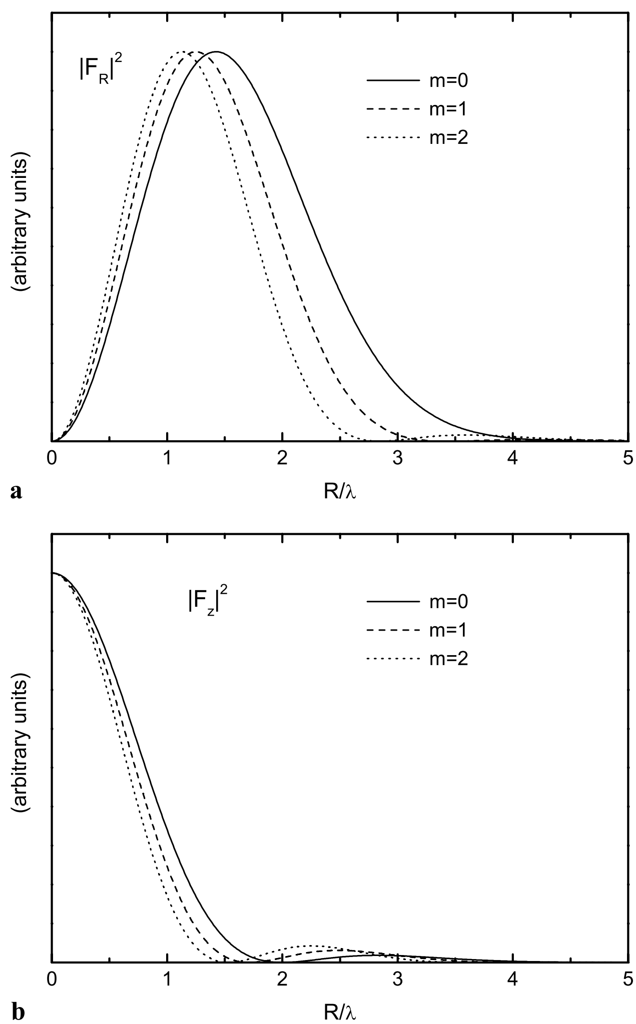

Fig. 5 Comparative plots of $|F_R|^2$ (**a**) and $|F_z|^2$ (**b**) at the initial transverse plane $z = 0$ for the function [see (11)] $f_0(\rho) = (\frac{\rho}{D})^m \exp(-\frac{\rho^2}{D^2})$, with $m = 0, 1, 2$

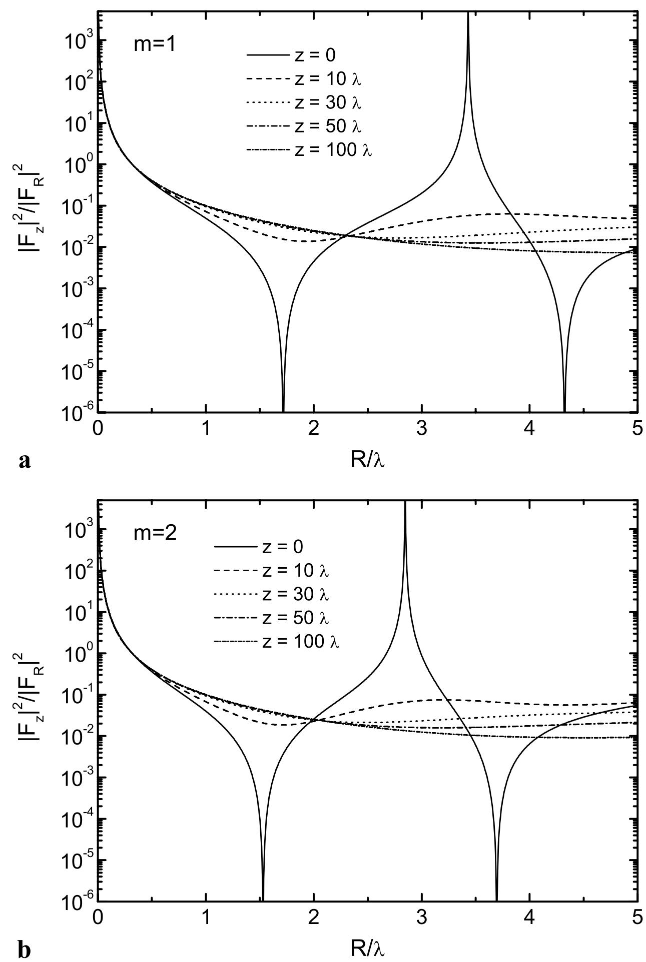

Fig. 6 The same as in Fig. 4 but now for $f_0(\rho)$ given by (17) with $m = 1$ (**a**) and $m = 2$ (**b**)

2. Under propagation into free space, the longitudinal polarization predominates within a transverse region close enough to the z-axis (say, $R \leq 0.4\lambda$).
3. As it was pointed out before (see Fig. 3), the longitudinal component at the initial plane is suppressed at a ring whose radius is 2λ. This does not occur after propagation.
4. All the curves cross at a certain point (radial value). This means that, near a transverse ring whose radius approaches 3λ, the ratio $\frac{|F_z|^2}{|F_R|^2}$ takes the same value for different propagation distances.

As a second example of interest, let us now consider in (11) the following function:

$$f_0(\rho) = \left(\frac{\rho}{D}\right)^m \exp\left(-\frac{\rho^2}{D^2}\right), \quad m = 1, 2. \tag{17}$$

Compared with the bell-shaped spectrum given by (16), the present case corresponds to a depleted-center function. Let us point out a number of differences with respect to the previous example.

Figure 5 shows and compares the relative strength of the radial and longitudinal components at the initial plane for the values $m = 0, 1, 2$. Although the global shape of the curves is qualitatively similar, we see, however, that the curve $|F_R|^2$ exhibits one zero out of the origin (Fig. 5a), i.e. the radial component vanishes on a certain ring. Recall that when $m = 0, |F_R|^2$ differs from zero at any point of the transverse plane $z = 0$ (except at the origin). Concerning $|F_z|^2$ (Fig. 5b), for the values $m = 1$ and $m = 2$ the longitudinal component is suppressed at two rings (in the pure Gaussian case [cf. (16)], $|F_z|^2$ equals zero for $R = 2\lambda$ only). Note also from these figures that the significant part of both components becomes more and more concentrated in the vicinity of the z-axis as m increases.

Figures 6a and b generalize the behavior of Fig. 4 for the values $m = 1$ and 2. The sharp peaks correspond to the zeros of $|F_R|^2$ and $|F_z|^2$. It is interesting to note that such zeros are reached at radial distances closer to the z-axis as m takes higher values.

6 Conclusions

Starting from a (hypothetical) purely longitudinal vectorial distribution at some transverse plane, it has been obtained the general propagation law of the field (exact solution of the Maxwell equations) that is (algebraically) closest to such a prescribed distribution. In the rotationally symmetric case, the above expression splits out as the sum of two terms, $iF_R\boldsymbol{u}_R$ and $F_z\boldsymbol{u}_z$, with radial symmetry and longitudinal polarization, respectively. This behavior reinforces the well-known possibility of enhancing the longitudinal component at the focal region by using radially polarized beams. Two special cases have been analysed, associated to bell-shaped and depleted-center functions, and their properties upon free propagation have been discussed. Apart from several differences we have mentioned, it has been found an overall qualitative similarity between the examples. This is an analytical consequence of the factors ρ^2 and ρ^3 inside the integrals providing, respectively, the radial and longitudinal components of the closest field [cf. (14)]. It should finally be remarked that the problem of finding prescribed distributions (other than Gaussian) that produce enhanced longitudinal components or sharper focusing is significant enough to deserve further study in the future.

Acknowledgements This work has been supported by the Ministerio de Educación y Ciencia of Spain, project FIS2007-63396.

References

1. B. Richard, E. Wolf, Proc. R. Soc. A **253**, 23 (1959)
2. Q. Lü, S. Dong, Horst Weber. Opt. Quantum Electron. **27**, 777 (1995)
3. R. Martínez-Herrero, P.M. Mejías, G. Piquero, *Characterization of Partially Polarized Light Fields* (Springer, Berlin, 2009)
4. D.P. Biss, T.G. Brown, Opt. Lett. **28**, 923 (2003)
5. E.Y.S. Yew, C.J.R. Sheppard, Opt. Commun. **275**, 453 (2007)
6. L. Novotny, M.R. Bebersluis, K.S. Youngworth, T.G. Brown, Phys. Rev. Lett. **86**, 5251 (2001)
7. B. Hayazawa, Y. Saito, S. Kawata, Appl. Phys. Lett. **85**, 6239 (2004)
8. E.J. Bochove, G.T. Moore, M.O. Scully, Phys. Rev. A **46**, 6640 (1992)
9. C.J.R. Sheppard, J. Opt. Soc. Am. A **18**, 1579 (2001)
10. R. Dorn, S. Quabis, G. Lenchs, Phys. Rev. Lett. **91**, 233901 (2003)
11. C.J.R. Sheppard, A. Choudhury, Appl. Opt. **43**, 4322 (2004)
12. H. Wang, L. Shi, B. Lukyanchuk, C.J.R. Sheppard, C.T. Chong, Nat. Photonics **2**, 501 (2008)
13. M. Meyer, V. Romano, T. Feurer, Appl. Phys. A **86**, 329 (2007)
14. D.G. Hall, Opt. Lett. **21**, 9 (1996)
15. P. Varga, P. Török, Opt. Lett. **21**, 1523 (1996)
16. S.R. Seshadri, J. Opt. Soc. Am. A **15**, 2712 (1998)
17. C.J.R. Sheppard, S.R. Seshadri, J. Opt. Soc. Am. A **16**, 1381 (1999)
18. C.J.R. Sheppard, J. Opt. Soc. Am. A **17**, 335 (2000)
19. A.V. Nesterov, V.G. Niziev, Phys. Rev. E **71**, 046608 (2005)
20. H.M. Guo, J.B. Chen, S.L. Zhuang, Opt. Express **14**, 2095 (2006)
21. G.Q. Zhou, L. Chen, Y.Z. Ni, Chin. Phys. Lett. **23**, 1180 (2006)
22. G.Q. Zhou, K.C. Zhu, F.Q. Liu, Opt. Commun. **276**, 37 (2007)
23. D.M. Deng, Q. Guo, Opt. Lett. **32**, 2711 (2007)
24. R. Martínez-Herrero, P.M. Mejías, S. Bosch, A. Carnicer, J. Opt. Soc. Am. A **18**, 1678 (2001)
25. R. Martínez-Herrero, P.M. Mejías, S. Bosch, Opt. Commun. **281**, 3046 (2008)
26. R. Martínez-Herrero, P.M. Mejías, Opt. Express **16**, 9021 (2008)